

Visual Tracking for Intelligent Vehicle-Highway Systems

Christopher E. Smith¹
chsmith@cs.umn.edu

Charles A. Richards²
richards@cs.stanford.edu

Scott A. Brandt³
sbrandt@cs.colorado.edu

Nikolaos P. Papanikolopoulos^{1*}
npapas@cs.umn.edu

¹Artificial Intelligence, Robotics, and Vision Lab
Department of Computer Science
University of Minnesota
4-192 EE/CS Building
200 Union St. SE
Minneapolis, MN 55455

²Stanford Vision Lab
114 Gates Building 1A
Stanford University
Stanford, CA 94305-9010

³Department of Computer Science
University of Colorado-Boulder
Campus Box 430
Boulder, CO 80309-0430

Accepted to the IEEE Transactions on Vehicular Technology

** Author to whom all correspondence should be sent.*

Visual Tracking for Intelligent Vehicle-Highway Systems

Christopher E. Smith

chsmith@cs.umn.edu

Artificial Intelligence, Robotics, and Vision Lab

Department of Computer Science

University of Minnesota

4-192 EE/CS Building

200 Union St. SE

Minneapolis, MN 55455

Scott A. Brandt

sbrandt@cs.umn.edu

Department of Computer Science

University of Colorado-Boulder

Campus Box 430

Boulder, CO 80309-0430

Charles A. Richards

richards@cs.umn.edu

Stanford Vision Lab

114 Gates Building 1A

Stanford University

Stanford, CA 94305-9010

Nikolaos P. Papanikolopoulos*

npapas@cs.umn.edu

Artificial Intelligence, Robotics, and Vision Lab

Department of Computer Science

University of Minnesota

4-192 EE/CS Building

200 Union St. SE

Minneapolis, MN 55455

ABSTRACT

The complexity and congestion of current transportation systems often produce traffic situations that jeopardize the safety of the people involved. These situations vary from maintaining a safe distance behind a leading vehicle to safely allowing a pedestrian to cross a busy street. Environmental sensing plays a critical role in virtually all of these situations. Of the sensors available, vision sensors provide information that is richer and more complete than other sensors, making them a logical choice for a multisensor transportation system. In this paper we propose robust detection and tracking techniques for intelligent vehicle-highway applications where computer vision plays a crucial role. In particular, we demonstrate that the Controlled Active Vision framework [15] can be utilized to provide a visual tracking modality to a traffic advisory system in order to increase the overall safety margin in a variety of common traffic situations. We have selected two application examples, vehicle tracking and pedestrian tracking, to demonstrate that the framework can provide precisely the type of information required to effectively manage the given traffic situation.

* Author to whom all correspondence should be sent.

1 Introduction

Transportation systems, especially those involving vehicular traffic, have been subjected to considerable increases in complexity and congestion during the past two decades. A direct result of these conditions has been a reduction in the overall safety of these systems. In response, the reduction of traffic accidents and the enhancement of an operator's abilities have become important topics in highway safety. Improved safety can be achieved by assisting the human operator with a computer warning system and by providing enhanced sensory information about the environment. In addition, the systems that control the flow of traffic can likewise be enhanced by providing sensory information regarding the current conditions in the environment. Information may come from a variety of sensors such as vision, radar, and ultrasonic range-finders. The sensory information may then be used to detect vehicles, traffic signs, obstacles, and pedestrians with the objectives of keeping a safe distance from static or moving obstacles and obeying traffic laws. Radar, Global Positioning System (GPS), and laser and ultrasonic range-finders have been proposed as efficient sensing devices. Vision devices (i.e., CCD cameras) have not been extensively used due to their high cost and noisy nature. However, the new generation of CCD cameras and computer vision hardware allows for efficient and inexpensive use of vision sensors as a component of a larger, multisensor system.

The primary advantage of vision sensors is their ability to provide diverse information on relatively large regions. Simple tracking techniques may be used with visual data taken from a vehicle to track several features of the obstacle ahead. This tracking allows us to detect obstacles (e.g., pedestrians, vehicles, etc.) and keep a safe distance from them. Optical flow techniques in conjunction with automatic selection of features allow for fast estimation of the obstacle-related parameters, resulting in robust obstacle detection and tracking with little operator intervention. In addition, surface features on the obstacles or knowledge of the approximate shape of the obstacles (i.e., the shape of the body of a pedestrian or automobile) may further improve the robustness of the tracking scheme. A single camera is proposed instead of a binocular system because one of our main objectives is to demonstrate that relatively unsophisticated and uncalibrated off-the-shelf

hardware can be used to solve the problem. The ultimate goal of this research is to examine the feasibility of incorporating visual sensing into an automated Intelligent Vehicle-Highway System (IVHS) that provides information about pedestrians, traffic signs, and other vehicles.

One solution to these issues can be found under the Controlled Active Vision framework [15]. Instead of relying heavily on *a priori* information, this framework provides the flexibility necessary to operate under dynamic conditions where many environmental and target-related factors are unknown and possibly changing. The Controlled Active Vision framework utilizes the Sum-of-Squared Differences (SSD) optical flow measurement [2] as an input to a control loop. The SSD algorithm is used to measure the displacements of feature windows in a sequence of images where the displacements may be induced by observer motion, target motion, or both. These measured displacements are then used as one of the inputs into an intelligent traffic advisory system.

Additionally, we propose a visual tracking system that does not rely upon accurate measures of environmental and target parameters. An adaptive filtering scheme is used to track feature windows on the target in spite of the unconstrained motion of the target, possible occlusion of feature windows, and changing target and environmental conditions. Relatively high-speed targets are tracked under varying conditions with only rough operating parameter estimates and no explicit target models. Adaptive filtering techniques are useful under a variety of situations, including the applications discussed in this paper: vehicle and pedestrian tracking.

We first describe some relevant previous research and present a detection scheme that focuses on computational issues in a way that makes a real-time application possible. Next, we describe our framework for the automatic detection of moving objects of interest. We then formulate the equations for measuring visual motion, including an enhanced SSD surface construction strategy and efficient search alternatives. We also discuss a feature window selection scheme that automatically determines which features are worthwhile for use in visual tracking. The paper continues with the presentation of the architecture that is used for conducting the visual tracking experiments. Furthermore, we document results from feasibility experiments for both of the

selected applications. Finally, the paper concludes with a discussion of the aspects of the system that deserve further consideration.

2 Previous Work

An important component of a real-time vehicle-highway system is the acquisition, processing, and interpretation of the available sensory information regarding the traffic conditions. At the lowest level, sensory information is used to derive discrete signals for a traffic or a vehicle system. There are many potential high-level uses for information that these lower levels can provide. Two common uses include automatic vehicle guidance and traffic management systems. For automatic vehicle guidance, a computer system assists or replaces the human's control of a vehicle. Traffic management systems require the information for reporting a traffic incident and/or altering traffic flow in order to correct the problem. In both of these cases, the system studies transportation conditions in order to adjust the behavior of a global information or control system.

Information about the traffic can be obtained through a variety of sensors such as radar sensors, loop detectors, and vision sensors. Among them, the most commonly used is the loop detector. However, loop detectors provide local information and introduce significant errors in their measurements. Recently, many researchers [7][8][10][11][12][16][18][20][22] have proposed computer vision techniques for traffic monitoring and vehicle control. Waterfall and Dickinson [21] proposed a vehicle detection system based upon frame differencing in a video stream. Houghton *et al.* [7] have proposed a system for tracking vehicles in video-images at road junctions. Inigo [8] has presented a machine vision system for traffic monitoring and control. A system that counts vehicles based on video-images has been built by Pellerin [16]. Kilger [11] has done extensive work on shadow handling in a video-based, real-time traffic monitoring system. Michalopoulos [12] has developed the Autoscope system for vision-based vehicle detection and traffic flow measurement. A system similar to the Autoscope traffic flow measuring system has been built by Takatoo *et al.* [18]. This system computes parameters such as average vehicle speed and spatial occupancy. A vision-based collision avoidance system has been proposed by Ulmer

[20]. Zielke *et al.* [22] have developed the CARTRACK system that automatically selects the back of vehicles in images and tracks them in real-time. In addition, similar car-following algorithms have been proposed by Kehtarnavaz *et al.* [10]. Finally, several other groups [5][19] have developed vision-based autonomous vehicles. In the remainder of this paper, we will highlight the differences of these approaches with the approach our work has taken.

3 Detection and Tracking in a Traffic Vision System

In general, the satisfaction of the goal of constructing visual tracking modalities for intelligent vehicle-highway systems requires the consideration of many elements. We have identified four principal categories of IVHS vision components. These include the detection of traffic objects of interest, the selection of features to be tracked, the tracking of features, and any motion or object analysis.

3.1 Detection of Traffic Objects of Interest

One limitation of tracking using feature windows based upon Sum-of-Squared Differences optical flow (see Sections 3.2 through 3.4) is that, by itself, there is no way of determining what the tracked feature represents. Considering only a window of intensities, we could be looking at a portion of a pedestrian, the edge of a building, a randomly-moving leaf, or a wide variety of other items. Given an arbitrary image, the success of tracking an object such as a pedestrian relies on the assumption that we somehow are able to detect that the tracked feature windows correspond to the object in question. Some research projects involved with the study of motion avoid this issue of detection by providing a human user with an interface for the selection of trackable features [15]. However, if an intelligent vision system is to be able to robustly track traffic objects in unpredictable, real-world environments, it is required that the system have some means of detecting such objects automatically.

In considering detection, it is helpful to consider an image to be comprised of pixels that are in one of two categories: *figure* or *ground*. Figure pixels are those which are believed to belong to a traffic object of interest, while ground pixels belong to the objects' environment. We consider

detection to be the identification and the analysis of figure pixels in each image of the temporal sequence.

There is a wide variety of techniques that could be used for the identification of whether a pixel is part of the figure or ground. For example, we could possess a model of the average shape of automobiles and attempt to fit this model to locations within an image. However, identification schemes that are computationally intensive may not be able to complete detection in real-time. Using such schemes would cause the vision system to lack robustness. In searching for a fast means to estimate the figure/ground state of a pixel, we consider the heuristic that uninteresting objects (such as a sidewalk) tend to be displayed by pixels whose intensities are constant or very slowly changing over time, while objects of interest (such as a pedestrian) tend to be located where pixel intensities have recently changed. Thus, a comparison between images that occurred at different times may yield information about the existence of important objects. This type of frame differencing has a long history in vehicle detection [21]. The work of Waterfall and Dickinson [21], for example, proposed frame differencing as a means for detecting vehicles in a sequence of images. Our system shares several ideas with their work, including a time averaged *ground image* and a filter to reduce artifacts caused by camera noise. Because of the limitations of processor speed when their work was published, they were unable to incorporate the filtering and the time averaged ground image in their system [21]. We have also extended this type of detection paradigm to include the use of detection domains, region merging, and post detection analysis directed at eliminating non-traffic related objects. These extensions are detailed in the remainder of this section.

The proposed scheme maintains a *ground image* that represents the past history of the environment. For each pixel in the current image, a comparison is made to the corresponding pixel in the ground image. If they differ by more than a threshold intensity amount, then the pixel is considered to be part of a binary *figure image*. If this threshold is too small, then portions of the object may blend into the background. If the threshold is too large, then slight changes in the environment will cause “false positive” errors in which the figure image contains many pixels that don’t

necessarily belong to important objects. A smaller, more sensitive threshold can be used if the images are preprocessed with a low-pass filter. The filter spatially averages the pixels, making camera noise cause smaller difference values. Experimentally, a 10% difference from a range of 256 grayscale intensity values was found to be a good general-purpose threshold level.

Figure 1 shows the construction of a figure image. The upper left window shows a portion of a ground image that has been stored in memory. The upper right window shows a corresponding portion of the current image. At the instant of time that was selected for this image, a pedestrian had just begun crossing the street. The lower window shows how the pedestrian becomes readily apparent, as the figure image is formed by comparing the current and the ground images.

Initially, the ground image is a copy of the first image of the sequence. However, environmental changes (e.g., moving clouds and the corresponding shadows) may cause a pixel's

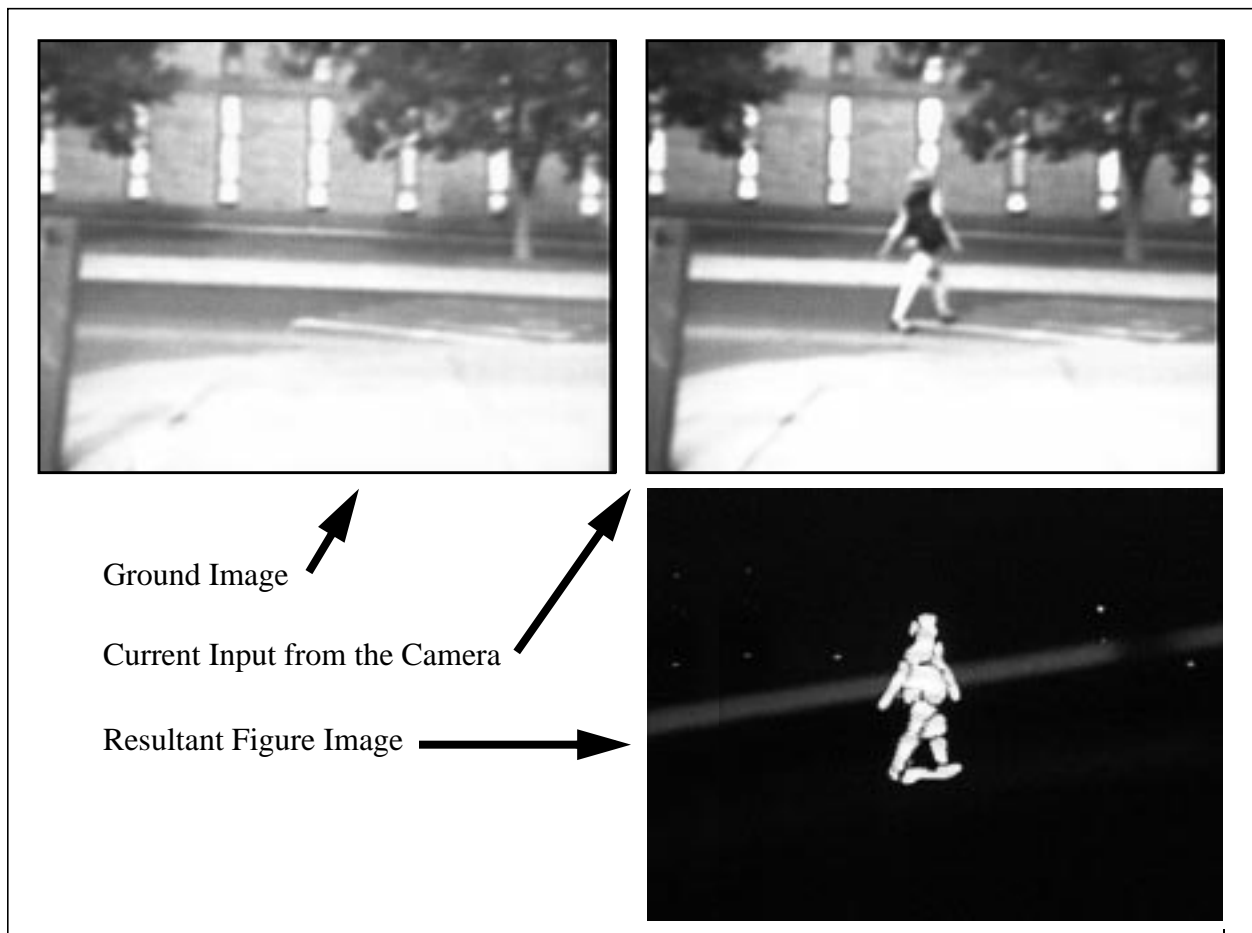


Figure 1: Figure Image Construction

intensity to vary over time. To account for this dynamic aspect of IVHS environments, our system periodically updates the ground image with information from the current frame of intensities. Rather than periodically replacing the previous ground image, a new ground image is produced by incorporating new intensity values from the current image according to:

$$G_i = (1 - \alpha)G_{i-1} + \alpha I_k \quad (1)$$

where G_i is the i th ground image ($i = k \bmod 3600$), I_k is the current image, and α ($0 \leq \alpha \leq 1$) is a scalar representing the importance of the current data. This equation refers to the intensities of a specific pixel location in both the ground image and the current image.

Once a figure image has been obtained, we can consider the other activity of detection: analyzing the traffic objects that may be present in the figure image. However, figure images tend to contain pixels that belong to a variety of items other than just the traffic objects of interest. For example, one may find objects such as vehicles in the pedestrian tracking domain, regions caused by shadows, and small areas of false detection caused by camera noise. The identification and removal of many of these problem cases occurs as a beneficial side-effect of the partitioning of figure pixels into *segments* that each represent a traffic object.

The image figure segmentation is achieved through a single pass of the Sequential Labeling Algorithm described in [6]. Because the algorithm creates segments from only a single pass through the binary figure image, all statistics that are to be calculated for the segments must be done dynamically. The selection of which statistics to calculate depends on the segment analysis; for our purposes it suffices to maintain a size (pixel count) and a bounding box of the minimum and maximum pixel locations in the two image dimensions (see Figure 2). There can be as many as several hundred segments generated in a single image, only a few of which describe traffic objects. Since the computational performance of object detection relies on keeping the number of considered segments to a minimum, several pruning steps must be performed. In particular, a pass is made through the segment data structure after each scanline is processed, during which many segments are pruned away if they are found to have different dimensions than those of a typical traffic object. In practice, this pruning removes almost all of the undesirable sources of figure



Figure 2: Segmentation Output

segments.

A common artifact that is observed with figure images is that objects will often be illuminated in a way that causes a curve of background-matching intensities along the interior of their projected area. For example, the arm of a pedestrian may sometimes be seen in the figure as two adjacent halves. The result is a pair of segments whose bounding boxes overlap. Since these curves are usually not parallel to an axis for their entire length, bounding box pairs caused by this phenomenon almost always overlap. Thus, overlapping figure segments are merged into a single bounding box, as illustrated in Figure 3.

Even though the figure/ground approach is a relatively fast form of object detection, its critical real-time nature is such that we would still like to identify ways in which the performance can

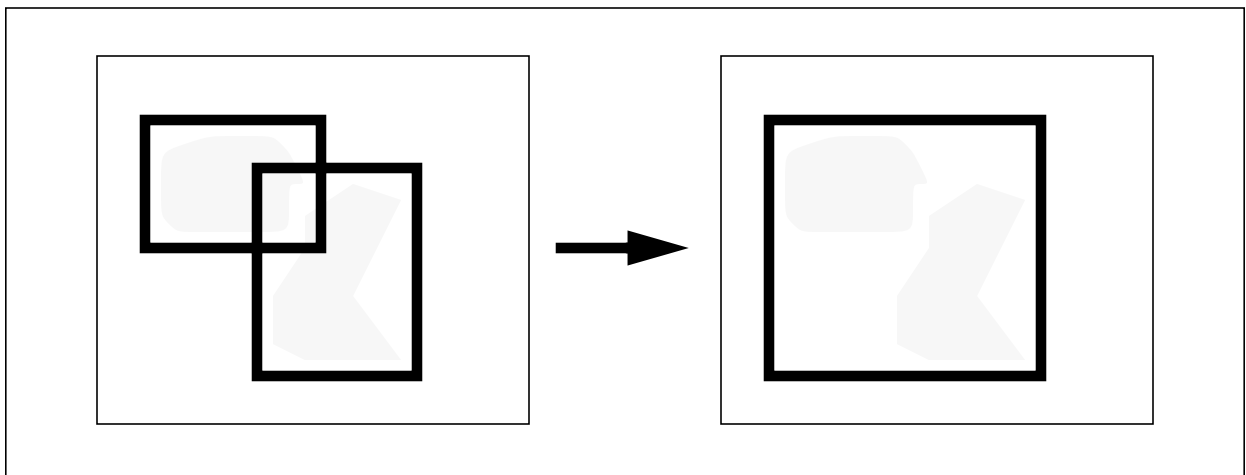


Figure 3: Segment Merging

be improved. One such method involves the use of *domains*. A domain is an individual, rectangular portion of the current image frame within which the segmentation algorithm is applied. Instead of using a single domain that covers the entire image, time can be saved by the appropriate use of several, smaller domains. The segments obtained from each domain are then combined into a resultant object set.

In our approach, there are two types of domains, *spontaneous* and *continuous*. Spontaneous domains are rectangular areas specified by a person as a part of configuring the system to a particular location. Spontaneous domains are placed where it is anticipated that a traffic object will appear for the first time. For example, pedestrian tracking with spontaneous domains may work best if the domains are placed close to the intersection of sidewalks and the boundaries of the image. Continuous domains for detection with a particular image are generated automatically by considering rectangular areas that are centered around the locations of segments in the previous iteration of detection. The continuous domains have dimensions that cause them to have slightly more pixels than the previously detected segments, in each dimension. Continuous domains allow for the efficient detection of mobile traffic objects at times when they move away from the spontaneous domain locations. Since spontaneous and continuous domains may overlap and it would be wasteful to perform segmentation repeatedly with the same pixels, intersecting domains are temporarily merged in a way that is similar to the merging of intersecting figure segments, as described above.

Once detected, the object of interest must be tracked. In the following sections, we describe the visual measurements we use to select and track features. The measurements are based upon the Sum-of-Squared Differences (SSD) optical flow [2].

3.2 Visual Measurements

Our goal is an IVHS sensing modality capable of measuring motion in a temporal sequence of images. This section includes the formulation of the equations for measuring this motion. Our vehicle and pedestrian tracking applications use the same basic visual tracking measurements that

are based upon a simple camera model and an optical flow measure. The visual measurements are combined with search-specific optimizations in order to enhance the visual processing from frame-to-frame and to optimize the performance of the system in our selected applications. Additionally, automatic selection of the features to be tracked is also based upon these equations for measuring motion.

3.2.1 Camera Model and Optical Flow

We assume a pinhole camera model with a world frame, \mathbf{R}_W , centered on the optical axis. In addition, a focal length f is assumed. A point $\mathbf{P} = (X_W, Y_W, Z_W)^T$ in \mathbf{R}_W , projects to a point \mathbf{p} in the image plane with coordinates (x, y) . We can define two scale factors s_x and s_y to account for camera sampling and pixel size, and include the center of the image coordinate system (c_x, c_y) given in frame F_A [15]. This results in the following equations for the actual image coordinates (x_A, y_A) :

$$x_A = \frac{fX_W}{s_x Z_W} + c_x = x + c_x \quad \text{and} \quad y_A = \frac{fY_W}{s_y Z_W} + c_y = y + c_y. \quad (2)$$

Any displacement of the point \mathbf{P} can be described by a rotation about an axis through the origin and a translation. If this rotation is small, then it can be described as three independent rotations about the three axes \mathbf{X}_W , \mathbf{Y}_W , and \mathbf{Z}_W [4]. We will assume that the camera moves in a static environment with a translational velocity (T_x, T_y, T_z) and a rotational velocity (R_x, R_y, R_z) . The velocity of point \mathbf{P} with respect to \mathbf{R}_W can be expressed as:

$$\frac{d\mathbf{P}}{dt} = -\mathbf{T} - \mathbf{R} \times \mathbf{P}. \quad (3)$$

By taking the time derivatives and using equations (2) and (3), we obtain:

$$\mathbf{u} = \frac{dx}{dt} = \left[x \frac{T_z}{Z_W} - f \frac{T_x}{Z_W s_x} \right] + \left[x y \frac{s_y R_x}{f} - \left(\frac{f}{s_x} + x^2 \frac{s_x}{f} \right) R_y + y \frac{s_y R_z}{s_x} \right] \quad (4)$$

$$\mathbf{v} = \frac{dy}{dt} = \left[y \frac{T_z}{Z_W} - f \frac{T_y}{Z_W s_y} \right] + \left[\left(\frac{f}{s_y} + y^2 \frac{s_y}{f} \right) R_x - x y \frac{s_x}{f} R_y - x \frac{s_x}{s_y} R_z \right]. \quad (5)$$

We use a matching-based technique known as the Sum-of-Squared Differences (SSD) optical flow [2]. For the point $\mathbf{p}(k-1) = (x(k-1), y(k-1))^T$ in the image $(k-1)$ where k denotes the k th

image in a sequences of images, we want to find the point $\mathbf{p}(k) = (x(k-1)+u, y(k-1)+v)^T$. This point $\mathbf{p}(k)$ is the new position of the projection of the feature point \mathbf{P} in image k . We assume that the intensity values in the neighborhood N of \mathbf{p} remain relatively constant over the sequence k . We also assume that for a given k , $\mathbf{p}(k)$ can be found in an area Ω about $\mathbf{p}(k-1)$ and that the velocities are normalized by time T to get the displacements. Thus, for the point $\mathbf{p}(k-1)$, the SSD algorithm selects the displacement $\Delta\mathbf{x} = (u, v)^T$ that minimizes the SSD measure

$$e(\mathbf{p}(k-1), \Delta\mathbf{x}) = \sum_{m, n \in N} [I_{k-1}(x(k-1) + m), y(k-1) + n) - I_k(x(k-1) + m + u, y(k-1) + n + v)]^2 \quad (6)$$

where $u, v \in \Omega$, N is the neighborhood of \mathbf{p} , m and n are indices for pixels in N , and I_{k-1} and I_k are the intensity functions in images $(k-1)$ and (k) .

In theory, the exhaustive search of the area Ω for an optimal SSD value is sufficient to visually track a particular feature window. In practice, however, there are three main problems that must be considered. First, if the motion of a traffic object is rapid enough to cause its projection to move beyond the bounds of the search area before the tracking algorithm is able to complete its search, then the algorithm will fail. Second, if we increase the size of the area Ω in an effort to reduce the likelihood of the previous problem, the time required for an iteration of tracking increases, possibly making the problem worse. Third, the image intensity values of the tracked object may change as the object experiences effects such as occlusion, non-rigid motion, and illumination changes.

The following section describes a method for addressing the first two problems. The method resolves the conflicting goals of searching a large area and of minimizing computations. Approaches are then discussed that improve the performance of the SSD search without requiring the reduction of the search area size.

3.2.2 Dynamic Pyramiding

Dynamic pyramiding is a heuristic technique which attempts to resolve the conflict between fast computation and capturing large motions. Earlier systems utilized a preset level of pyramid-

ing to resolve this conflict, at the expense of tracking accuracy [15]. In contrast, dynamic pyramiding uses multiple levels of pyramiding (see Figure 4). The level of the pyramiding is selected based upon the observed displacements of the target’s feature windows. If the displacements are small relative to the search area, the pyramiding level is reduced; if the measured displacements are large compared to the search area, then the pyramiding level is increased. This results in a system that enhances the tracking speed when required, but always biases in favor of the maximum accuracy achievable. The dynamic level switching thus allows the tracker to adjust to accelerations of the target (when displacements increase) and then to increase accuracy when the target is at rest. The system is capable of capturing large motions without incurring additional computational overhead, while maintaining accuracy when possible.

During the search process, the SSD measurements are centered upon particular positions in the pyramided search area. Which positions are selected ($\Delta \mathbf{x} = (\mathbf{u}, \mathbf{v})^T$ in equation (6)) is dependent upon which of the four levels of pyramiding is currently active. The lowest level searches every position in a square 32×32 pixel patch of the current frame. The second level searches every other position in a 64×64 patch, and the third, every third position in a 96×96 patch. The fourth and highest level searches every fourth position in a 128×128 patch.

Dynamic pyramiding provides the flexibility required when the objects of interest are moving at high speeds relative to the image plane. In some of our applications (for instance, vehicle following), the object of interest may be traveling at speeds of up to 65 miles per hour, but the

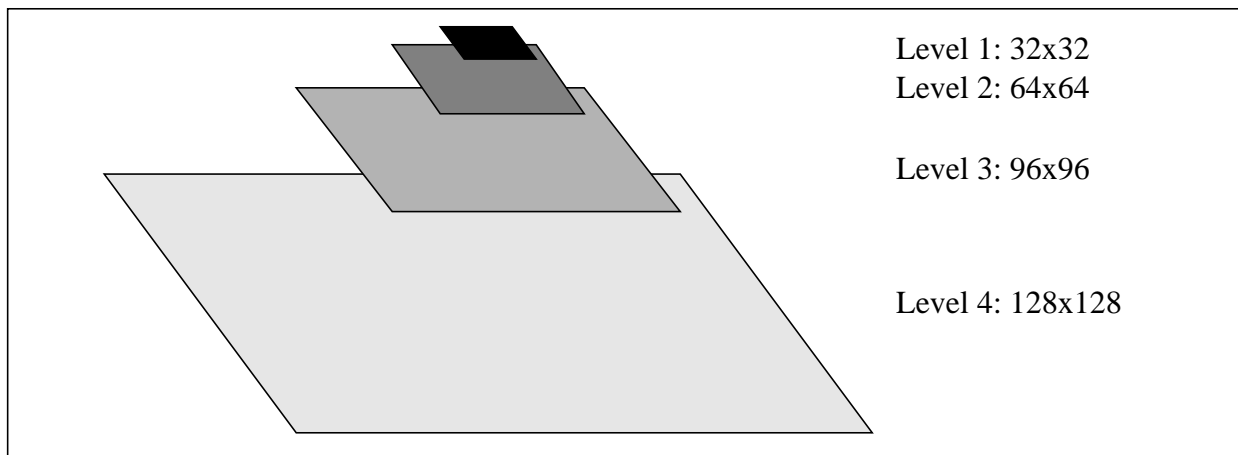


Figure 4: Dynamic Pyramiding

speed relative to the image plane is quite low. In other cases (e.g. pedestrian tracking or vehicle lane changes), the speed of the object relative to the image plane may be quite high. In these cases, dynamic pyramiding compensates for the speed of the features on the image plane, allowing the system to maintain object tracking.

3.2.3 Loop Optimizations

We now consider a means of reducing tracking latency without decreasing the neighborhood size. The primary source of latency in a vision system that uses the SSD measure is the time needed to identify the minimizing $(u, v)^T$ in equation (6). To find the true minimum, the SSD measure must be calculated over each possible $(u, v)^T$. The time required to produce a SSD surface and to find its minimum can be greatly reduced by employing a loop short-circuiting optimization. During the search for the minimum on the SSD surface (the search for $(u, v)_{min}^T$), the SSD measure must be calculated according to equation (6). This requires nested loops for the m and n indices. During the execution of these loops, the SSD measure is calculated as the running sum of the squared pixel value differences. If the current SSD minimum is checked against the running sum as a condition on these loops, the execution of the loops can be short-circuited as soon as the running sum exceeds the current minimum. This optimization has a worst-case performance equivalent to the original algorithm plus the time required for the additional condition tests. This worst case occurs when the SSD surface minimum lies at the last $(u, v)^T$ position searched. On average, this type of short-circuit realizes a decrease in execution time by a factor of two.

Another means for reducing latency for a given neighborhood size is based upon the heuristic that the best place to begin the search is at the point where the minimum was last found on the surface, expanding the search radially from that point. This heuristic works well when the disturbances being measured are relatively regular and small. In the case of tracking, this corresponds to targets that have locally smooth velocity and acceleration. If a target's motion does not exhibit such relatively smooth curves, then the target itself is fundamentally untrackable due to the inherent latency in the video equipment and the vision processing system.

Under this heuristic, the search pattern in the (k) image is altered to begin at the point on the SSD surface where the minimum was located for the ($k - 1$) image. The search pattern then spirals out from this point, searching over the extent of u and v . This is in contrast with the typical indexed search pattern where the indices are incremented in a row-major scan fashion. Figure 5 contrasts a traditional row-major scan and the proposed spiral scan where the center position corresponds to the position where the minimum was last found. This search strategy may also be combined with a predictive filter to begin the search for the SSD minimum at the position that the predictive aspect of the filter indicates to be the possible location of the minimum.

Since the structure that implements the spiral search pattern contains no more overhead than the loop structures of the traditional search, worst-case performance is identical. In the general case, search time is approximately halved.

We observed that search times for feature windows varied significantly — by as much as 100 percent — depending upon the shape/orientation of the feature and the direction of motion. In determining the cause of this problem and exploring possible solutions, we realized that by applying the spiral image traversal pattern to the calculation of the SSD measure we could simultaneously fix the problem and achieve additional performance improvements. Spiraling the calculation of the SSD measure yields independence of best-case performance from the orientation and motion of the target by changing the order of the SSD calculations to no longer favor one

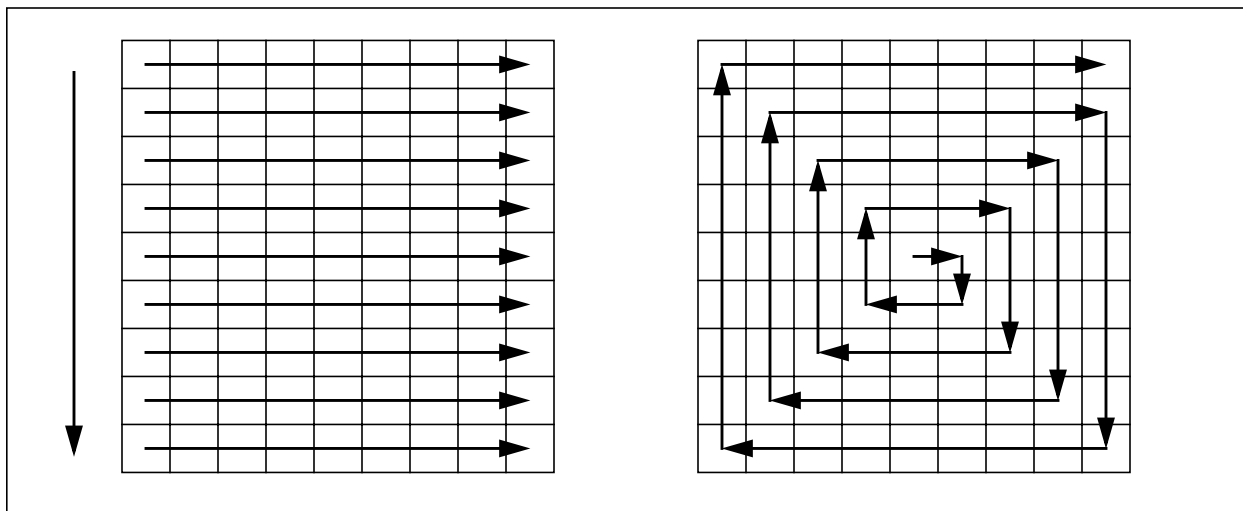


Figure 5: Traditional and Spiral Search Patterns

portion of the image over another. In the traditional calculation pattern (a row-major traversal of the feature region), information in the upper portion of the region is used before that in the lower portion of the region, thus skewing the timing in favor of those images where the target and/or foreground portion of the feature being tracked is in the upper half of the region and where the motion results in intensity changes in the same region. Additional speed gains are achieved because the area of greatest change in the SSD measure calculations typically occurs near the center of the feature window, which generally coincides with an edge or a corner of the target, resulting in fewer calculations before the loop is terminated in non-matching cases. Speed gains from this optimization are approximately 40%.

3.2.4 Greedy, Gradient-Following Neighborhood Search

Both the traditional indexed search patterns and the above-described spiral search variations perform an exhaustive computation over the feature window's entire neighborhood. While this exhaustive search is required in order to find the true SSD minimum, it may be desirable to sacrifice this guarantee in favor of expanding the search area Ω while the search time is kept low. This selects a point on the SSD surface that may not always be ideal, but can generally be found faster than an exhaustive search in an expanded Ω . This is done by only computing SSD values on a select few locations in the neighborhood, based on the SSD surface gradient information that previous computations may have provided. Imagine this search problem as one where you are located on an uncharted three-dimensional terrain and the goal is to locate the lowest point. If enough surface charting has taken place to indicate a depression, then it would make sense to continue charting in the direction of the depression. Further description of gradient-following search strategies can be found in [3].

The greedy search optimization begins at a location within the SSD surface, and it consists of a series of locally optimal *greedy* decisions. Each decision computes the SSD values of neighboring locations and selects the minimum. At the selected location, the same decision process is repeated until no neighboring SSD value is better than the current one. However, this algorithm provides no guarantees against instances of ridge, plateau, and foothill problems [3]. The greedy

searching optimization is typically able to compensate for the decrease in confidence in the selected $(\mathbf{u}, \mathbf{v})^T$ value by virtue of its speed.

3.3 Selection of Features to be Tracked

By computing a bounding box around a traffic object of interest (see Section 3.1), we have reduced the problem of locating trackable features in the entire image to the problem of locating trackable features in a smaller, rectangular region. We make the reasonable assumption that most possible feature selections made from within a bounding box either lie entirely within the object or contain at least a portion of the object's pixels. By selecting several features for each object, we increase the odds that we have a feature window on the object. Furthermore, our system tends to select features that are near the center of the bounding box, an area with even greater likelihood of being connected to the object.

But it is not enough to select any possible placement of a feature window within the bounding box of a figure object. The reason for this is because a visual tracking algorithm based upon the SSD technique may fail due to repeated patterns in the image's intensity function or due to large areas of uniform intensity. Both situations can provide multiple matches within a feature window's neighborhood, resulting in spurious displacement measures. In order to avoid this problem, our system considers and evaluates many candidate placements of a feature window. Candidate placements which correspond to unique features are automatically selected.

The feature window selection uses the SSD measure combined with an auto-correlation technique to produce a complete SSD surface corresponding to an auto-correlation in the area Ω [2][15]. Several possible confidence measures can be applied to the surface to measure the suitability of a potential feature window.

The selection of a confidence measure is critical since many such measures lack the robustness required by changes in illumination, intensity, etc. We utilize a two-dimensional displacement parabolic fit that attempts to fit parabola $e(\Delta\mathbf{x}_T) = a\Delta\mathbf{x}_T^2 + b\Delta\mathbf{x}_T + c$ to a cross-section of the surface derived from the SSD measure [15]. The parabola is fit to the surface pro-

duced by equation (6) at several predefined orientations. A feature window's confidence measure is defined as the minimum of these directional measures.

Naturally, several candidate feature windows are tested and those which result in the best confidence measures are kept. What remains to be discussed is the decision of which placements of feature windows are used as candidates. The feature selection algorithm does this by using another greedy, gradient-following search strategy. Depending on the number of desired resultant feature window selections, several searches are begun at pre-determined locations within the bounding box. A natural choice for at least one of these searches is the box's center. Confidence measures are computed for both the current candidate as well as for all the neighboring candidates. As before, search continues from the neighbor with the best result, until no neighboring confidence measures are better than the current one.

3.4 Feature Tracking and Motion Analysis

At this stage, the visual tracking system is provided with a set of features that it can track according to the SSD optical flow method described earlier. The system performs several iterations of the tracking phase, after which it returns to repeat the detection and selection steps. Thus, the goal of tracking feature windows can be considered as that of providing feature trajectories over time.

By advancing the capabilities of the IVHS visual tracking modality from the tracking of feature windows to the higher level of processing objects, we have provided the groundwork for a variety of possible analysis tasks. Some tasks that have potential traffic-related applications involve the identification of object characteristics such as the size of a pedestrian or the class of a vehicle. Other tasks include the identification of motion characteristics such as a pedestrian's gait or the time that the person takes to traverse an intersection.

4 The Minnesota Vision Processing System

The purpose of this section is to describe the architecture on which we have developed our visual tracking prototype. This description is intended to provide a justification for the way in

which our proposed algorithms address real-world constraints (e.g., complexity, accuracy, and robustness).

The Minnesota Vision Processing System (MVPS) used in these experiments is the image processing component of the Minnesota Robotic Visual Tracker (MRVT) [17] (see Figure 6). The MVPS receives input from a video source such as a camera mounted in a vehicle, a static camera, stored imagery played back through a Silicon Graphics Indigo, or a video tape recorder. The output of the MVPS may be displayed in a readable format or can be transferred to another system component and used as an input into a control subsystem. This flexibility offers a diversity of methods by which software can be developed and tested on our system. The main component of the MVPS is a Datacube MaxTower system consisting of a Motorola MVME-147 single board computer running OS-9, a Datacube MaxVideo20 video processor, and a Datacube Max860 vector processor in a portable 7-slot VME chassis. The MVPS performs the image processing computation and calculates any desired control input. It can supply the data or the input via shared memory to an off-board processor via a Bit-3 bus extender for inclusion as an input into traffic or vehicle control software. The video processing and calculations required to produce the desired control input are performed under a pipeline programming model using Datacube's Imageflow

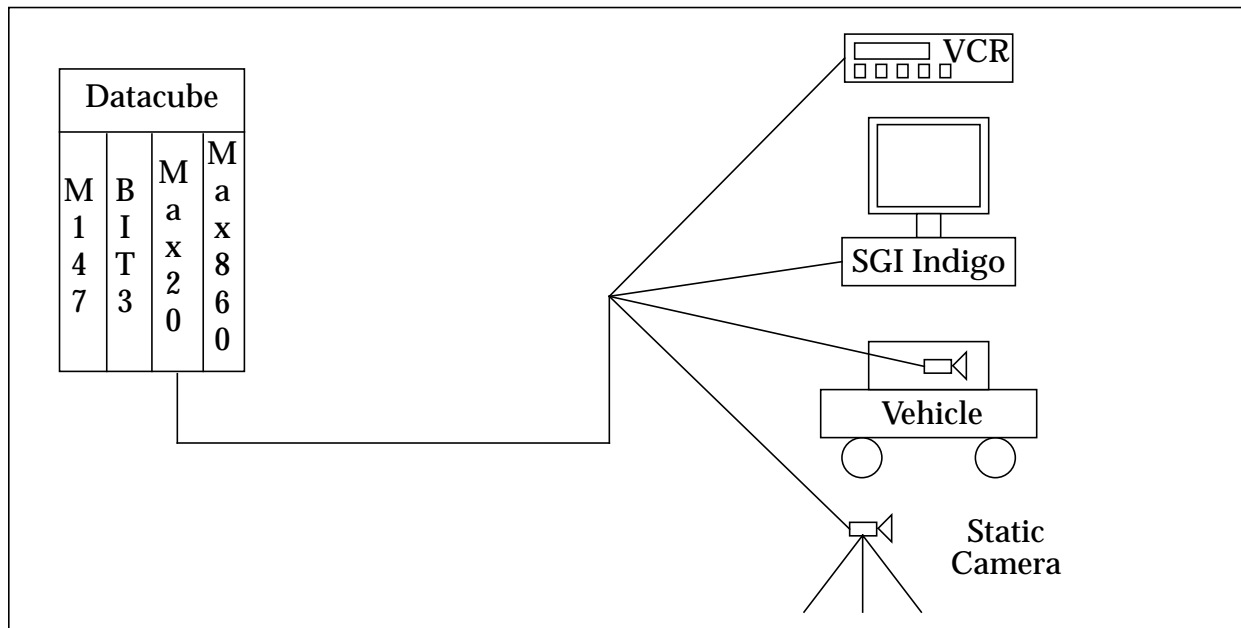


Figure 6: MVPS Architecture

libraries.

The speed at which visual information can be processed is generally an important consideration in the determination of the feasibility of computer vision systems. In the MVPS configuration, portions of a vision application that cannot be directly implemented with MaxVideo20 hardware elements can be programmed in software that runs on the Max860 processor. This processor has a peak performance rate of 80 Mflops. Communication between the MaxVideo20 and the Max860 occurs at 20 Mhz through the use of the P2 bus.

5 Experimental Results

5.1 Pedestrian Tracking

Pedestrians constitute one class of trackable objects that are of extreme importance to many IVHS applications. Considering the potential for injury when pedestrians and vehicles interact harmfully, the ability to track pedestrians is likely to be an important element of any visual tracking system that is used for IVHS applications. Pedestrian tracking was therefore selected as the first area to which our tracking paradigm was applied. In these experiments we consider the tracking of a pedestrian at an intersection by a static camera. By tracking pedestrians at intersections, data can be collected regarding the existence of pedestrians in the crosswalk, the crossing time of average pedestrians, and the identification of impaired pedestrians that cannot cross in the average time frame. This information can be used for intelligent signal control that adapts to the time required by impaired pedestrians to cross the street or for collaborative traffic/vehicle management systems.

The goal of the first experiments was to demonstrate that our methods could successfully track a pedestrian under normal environmental situations. The experiments consisted of a single pedestrian crossing a street at a controlled intersection (See Figure 7). The camera was mounted on the opposite side of the street in a position that was consistent with a mounting position on the utility pole supporting the intersection's crosswalk signals. Imagery was captured from a real intersection using a camcorder and was later input into the MVPS using a video cassette recorder.

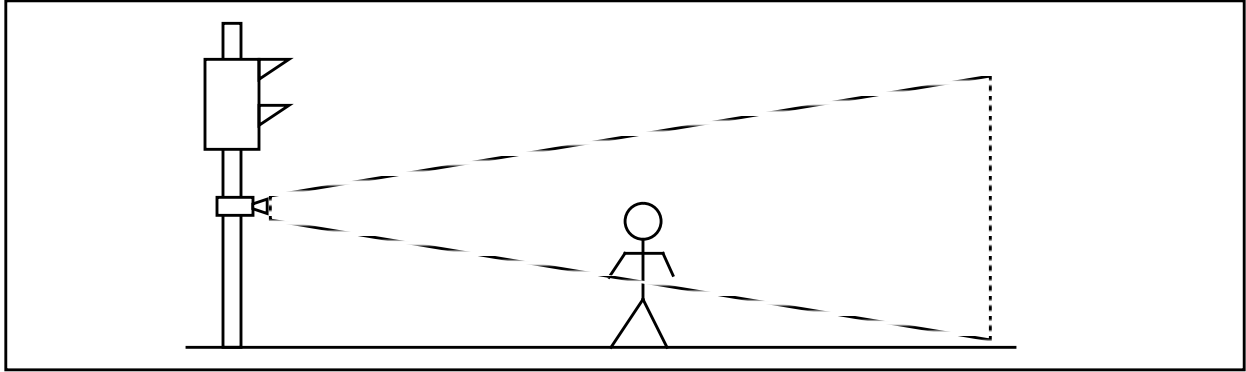


Figure 7: Experimental Setup

A single pedestrian crossed the street at the crosswalk, moving toward the camera (see Figure 8). Six example frames from a set of one hundred fifty frames of the pedestrian tracking appear at the end of this paper (see Figure 14, at the end of this paper). The system tracked a feature on the pedestrian (the contrast gradient at the pedestrian's waist). Target tracking was not lost during the duration of the crossing, in spite of the degraded contrast in the imagery due to an over-cast sky.

With the traditional application of optical flow tracking (described in Section 3.2.1), these results would have been difficult. However, by combining the loop short-circuiting, the spiral pattern for the search loop, and the spiral pattern for the SSD calculation loop (described in Section 3.2.3), we were able to find the minimum of an SSD surface as much as 17 times faster on the average than the unmodified search. Experimentally, the search times for the unmodified algorithm averaged 136 msec over 5000 frames under a variety of relative feature window motions. The modified algorithm with the search-loop short-circuiting alone averaged 60-72 msec search



Figure 8: Pedestrian Tracking

times over several thousand frames with arbitrary relative feature window motion. The combined short-circuit/spiral search algorithm produced search times which averaged 13 msec under similar tests and the combined short-circuit, dual-spiral algorithm produced search times which were as low as 8 msec. Together these optimizations allow the MVPS to track three to four features at RS-170 video rates (33 msec per frame) without video under-sampling. Subsequently, we applied the gradient-following search scheme to sample image sequences and performance was found to be similar to that for the combined short-circuit, dual-spiral algorithm.

The elements of the figure/ground system described earlier in the paper were implemented with success, considering that this application is still in the early stage of development. Using the pipeline image processing features of the Datacube MaxTower, the differencing between the current and ground images was done at frame-rate. The segmentation of a single test object (200 by 300 pixels) in a complete image (512 by 480 pixels) took 150 msec. This time was clearly reduced through the use of multiple, smaller domains. On an image sequence of several minutes of actual pedestrian traffic on a sidewalk, the system successfully followed every pedestrian who entered in the camera's field of view. That is, no false negatives occurred for the duration of the experiment. False positives did occur infrequently resulting in approximately 3% of the detections being incorrect after the completion of the segment merging and object analysis. In general, these occurred when a shadow of the traffic object fell on an object belonging to the ground image. One advantage of using a figure image for tracking traffic objects is that the technique can track multiple objects without a significant increase in computation. At the end of this paper there is a series of illustrations that demonstrate how two bounding boxes produced by the segmentation of figure images simultaneously track two pedestrians (see Figure 16).

The interaction between spontaneous and continuous domains substantially improved the effectiveness of the detection phase. In Figure 9, the dynamic nature of the domains is illustrated. First, the user selects two small domains at the ends of a sidewalk. Once the selection is made, only a small area of the intersection's projection is considered for segmentation of the figure image. In the lower left window, we see that the segmentation has identified a pedestrian who has

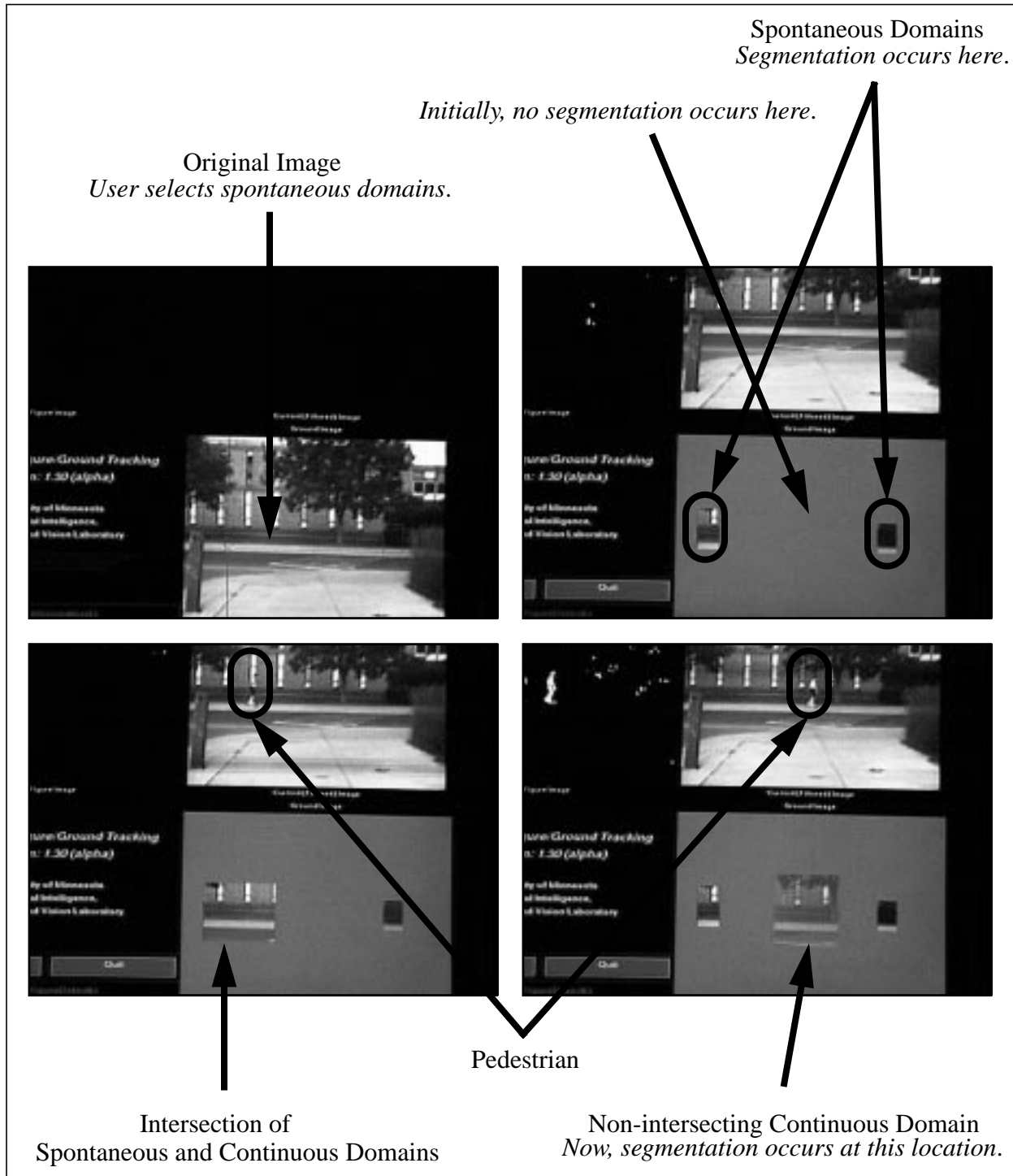


Figure 9: Segmentation Domains approached from the left. The continuous domain around the discovered pedestrian is intersected with the spontaneous domain that was already there. Finally, the lower right window shows the pedestrian having moved away from the spontaneous domain, causing there to be three separate

areas of figure segmentation.

5.2 Vehicle Tracking

A primary requirement of an intelligent vision system is that it must be able to detect and track potential obstacles. Of particular interest are other vehicles moving around and in front of the vehicle upon which the sensor is mounted (the primary vehicle). These vehicles constitute obstacles that must be avoided (collision avoidance) or a target that is to be followed (convoying).

Collision avoidance of moving vehicles (with a relatively constant velocity) detected near the primary vehicle can be effected with careful path planning. The basic goal is to maintain the desired speed and path (i.e., staying in the same lane of the road or highway) while avoiding other vehicles. Under normal circumstances this means accelerating and decelerating appropriately to avoid cars in front of and behind the primary vehicle. In extreme cases this means taking evasive action or warning the operator of a potential collision situation.

Another application area that involves the same basic problems is vehicle convoying. In this case, all path planning is done by the operator of the vehicle at the head of the convoy and all other vehicles must follow at a specified distance in a column behind the primary vehicle. For these reasons we chose to apply the Controlled Active Vision framework to the problem of tracking vehicles moving in roughly the same direction as the primary vehicle.

The experimental data was collected by placing a camcorder in the passenger seat of a car and driving behind other cars on the freeway (see Figure 10). This produced data that closely matched that which could be expected in a typical IVHS application. This data was later played back through a VCR and used as input to the MVPS, which tracked the vehicles and produced a series of (x, y) locations specifying the detected locations of the features being tracked. Because the exact world coordinate locations of the features in each frame of the video are unknown, we were unable to provide a complete analysis of the tracking performance of the system. However, a simple assumption about the motion of the vehicle in the frame yields conclusive results that match the intuitive results gained from viewing the graphic display of the vehicle tracking

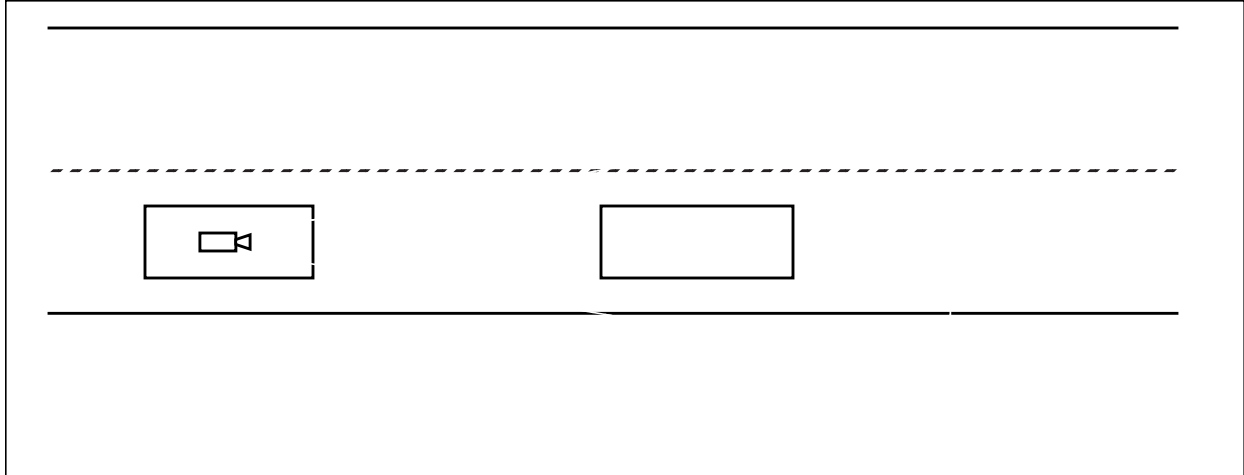


Figure 10: Experimental Setup

algorithm.

The MVPS includes a monitor upon which graphic representations of the tracking algorithm are displayed. While the system is tracking, the input data is displayed and a red box is drawn around the tracked location of the feature (see Figure 11). Initial experiments were done by watching the system track the features as they were displayed on the monitor. This allowed us to gain an understanding of the performance of the system under varying conditions and with a variety of features. In particular, we discovered that the performance of the system is very sensitive to the robustness of the features selected.

After initial studies were completed, we proceeded to do a quantitative analysis of the vehicle tracking performance. While we were unable to compare the tracking results against ground-truth data (exact locations of objects/features manually calculated off-line), we were able to pro-



Figure 11: Vehicle Tracking

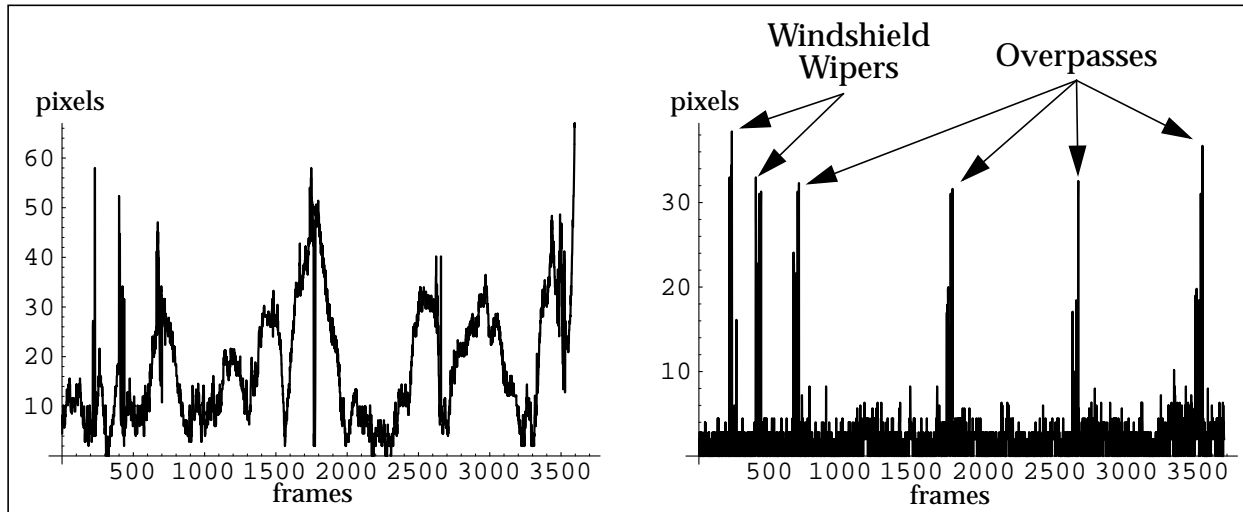


Figure 12: Licence Plate Results

vide a reasonable determination of the system performance by assuming that the motion of the vehicle within the frame would be relatively smooth and within easily determinable velocity bounds. In other words, any sufficiently large, quick motions of the tracked location were likely to be the result of a loss of tracking rather than due to motion of the vehicle. This hypothesis was confirmed by viewing the tracking results and correlating the spikes in the plots of the tracked locations with the motion of the displayed tracking windows.

Figure 12 shows the results of one such experimental run where a single feature (the license plate) was tracked on the back of a single vehicle that was followed for approximately 2 minutes. The plot on the left shows the motion of the feature in the frame with respect to a reference point in the image that corresponds to an initial location of the feature. The plot on the right shows the first derivative of the plot on the left. This plot clearly shows the relatively regular motion of the calculated feature position, corresponding to the relatively smooth motion of the tracked vehicle relative to the vehicle carrying the sensor. The spikes in the plot correspond to the times when the tracking was lost and the tracking window rapidly moved off the feature. The plot has been annotated to indicate the cause of the tracking problems, that in all cases were due to either momentary occlusion of the tracked feature by windshield wipers on the primary vehicle, or extreme changes in the relative brightness and contrast of the tracked feature as a result of the vehicles passing under overpasses on the freeway. In all cases tracking resumed immediately after the visual distur-

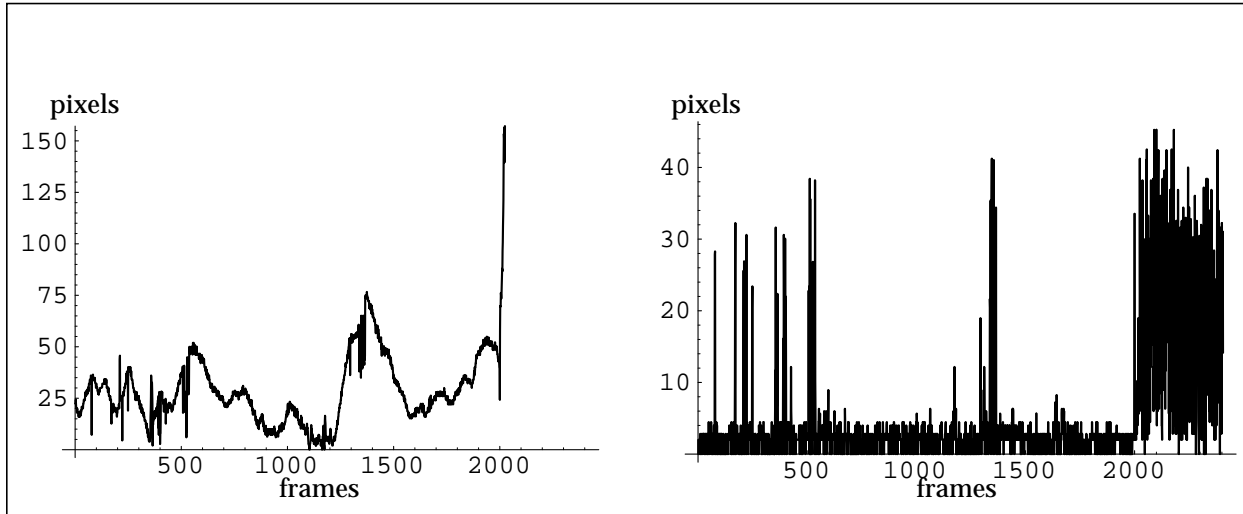


Figure 13: Spoiler Results

bance ended. In real-time this corresponded to less than a second of lost tracking per occurrence. Simple filtering techniques (e.g., Kalman filtering) would effectively remove virtually all perturbation of the tracking window resulting from such events.

Six selected frames of the test are presented in Figure 15 at the end of this paper. The image labeled “(d)” is taken just prior to the loss of tracking due to windshield wiper occlusion. The blur due to the wiper is just appearing in the lower left of the frame.

Figure 13 shows the results of tracking a different feature (the spoiler) on back of the same vehicle tracked in the previous example. Tracking performance in this example is considerably worse than in the previous example due to the poor SSD surface characteristics of the feature selected by the operator. The tracking exhibits problems similar to the previous example, but longer in duration and fails completely at about frame 2000. This failure corresponds to the algorithm finding a suitable feature match on the surface markings of the freeway. Automatic feature selection techniques presented earlier in this paper would not have chosen this feature for tracking due to its poor SSD surface characteristics.

6 Drawbacks and Potential Extensions

In researching the MVPS, several limitations or future problems became apparent. Drawbacks of relying solely upon the cross-correlated feature window tracking were previously

discussed, but the additional functions added to the visual system possess limitations as well. A clear example of one of these is the sensitivity of the detection phase to jitter in the visual input device. Unless the acquisition portion of the visual system contains sufficient stabilization abilities, even slight jolts or gusts of wind have the ability to shift the placement of projected items of the environment. This shifting causes large quantity of figure pixels along their borders. If we properly tune the predication of a figure segment being an acceptable representation of a traffic object of interest, then most of these large blobs of figure segments caused by camera jitter will be properly ignored. However, two problems still remain. First, performance suffers due to the larger number of pixels that are being processed at the time of the jitter. Second, objects that may otherwise have been detected could have their bounding boxes intersected with those caused by jitter, causing their undesirable removal.

Another concern that demands further research with the figure/ground approach is its dependence on environmental conditions. Some conditions that would disturb humans, such as heavy snowfall, would be ignored by the system (because each flake would be removed by the segmentation size thresholds). A relatively frequent example of environmental effects on traffic vision systems is that of cloud motion. Moving clouds can cause large, undesired regions in the figure image due to sharp illumination changes. Currently, such regions are dealt with in the same manner as those resulting from camera jitter.

Shadow handling is a common problem for most techniques that deal with the analysis of moving objects. With visual tracking, shadows are one of several sources (in addition to non-rigid motion, specular reflectivity, and others sources) for the variation in a feature window's intensity pattern. If this variation becomes too severe, the feature window will no longer be useful for estimating the motion of its associated object of interest. Our system partially compensates for shadows by continually switching between detection and tracking; however, the robust handling of the effects of shadows continues to be an open problem and part of our ongoing research.

Another issue for further improvement is the update of the ground image through the time-averaging process. Segmentation information can be used to increase the quality and the computa-

tional performance of the averaging. For example, information about the previous figure images can be used to limit the scope of the averaging to those pixels that lie outside the figure image.

Occasionally a traffic object of interest will occlude something in the background in such a way that corresponding colors for the two objects have hues that are clearly different to the human observer, but whose intensity values are similar. Performing the differencing portion of obtaining a figure image with more than just grayscale information may provide better results, but it adds computational and hardware costs.

The performance of the pedestrian tracking could possibly be enhanced with the use of explicit representations of people that are more complicated than simple bounding box constraints. A likely form would be to model a human as a semi-rigid body that deforms in known and predictable ways. Such tracking would allow the system to track pedestrians in spite of rapidly changing conditions (i.e., the pedestrian moving from shadow to bright light) and clutter in the image. Additionally, occlusion (due to a passing vehicle, other pedestrians, etc.) could be handled more robustly than it currently is. The method presented here may be used to track multiple features that in turn define the control points for a “snake,” or active deformable model, such as has been described by Kass [9].

Since the largest source of latency in the figure/ground approach (as implemented on the current hardware) lies in the switching between detection phase and the other phases, one might consider tracking traffic objects based on a efficient connection between figure segments from temporally adjacent frames. This would probably require the research of optimized correspondence schemes that were specific to a particular IVHS task.

Finally, we should remember that a large-scale IVHS project would likely have a visual tracking system as only one of many components. There are interesting challenges that deal with the incorporation of the visual sensing data into larger, multisensor application systems for various transportation applications.

7 Conclusion

This paper presents techniques for visual sensing in uncalibrated environments for intelligent vehicle-highway systems applications. The techniques presented provide ways of recovering unknown environmental parameters using the Controlled Active Vision framework [15]. In particular, this paper presents novel techniques for the automatic detection and visual tracking of vehicles and pedestrians.

For the problem of visual tracking, we propose a technique based upon earlier work in visual servoing [14][15] that achieves superior speed and accuracy through the introduction of several performance enhancing techniques. The method-specific optimizations also enhance overall system performance without affecting worst-case execution times. These optimizations apply to various region-based vision processing applications and, in our application, provide the speedup required to increase directly the effectiveness of the real-time vision system.

Progress toward the goal of real-time processing for intelligent vehicle-highway systems was also made by proposing means for performing other important visual motion tasks. A fast strategy was described for the detection of areas that deserve continued processing. We then showed how these areas of interest could then be used for the selection, tracking, and analysis of feature windows. Experimentation confirmed the plausibility of a system that follows this type of framework.

The application of these techniques to two selected IVHS problems has demonstrated the feasibility of using a vision sensor to derive salient information from real imagery. The information may then be used as an input into intelligent control or advisory systems. In such a system, vision would constitute only one of the sensing modalities available to the system. Other sensors such as radar, laser and ultrasonic range-finders, infra-red obstacle detectors, GPS, Forward Looking Infra-Red (FLIR), microwave, etc. may provide other modalities with particular strengths and weaknesses.

8 Acknowledgments

This work has been supported by the Minnesota Department of Transportation through Contracts #71789-72983-169 and #71789-72447-159, the Center for Transportation Studies through Contract #USDOT/DTRS 93-G-0017-01, the National Science Foundation through Contracts #IRI-9410003 and #IRI-9502245, the Army High Performance Computing Research Center under the auspices of the Department of the Army, Army Research Laboratory cooperative agreement number DAAH04-95-2-0003/contract number DAAH04-95-C-0008 (the content of which does not necessarily reflect the position of the policy of the government, and no official endorsement should be inferred), the Department of Energy (Sandia National Laboratories) through Contracts #AC-3752D and #AL3021, the McKnight Land Grant Professorship Program at the University of Minnesota, and the Department of Computer Science of the University of Minnesota.

9 References

- [1] T. Abramczuck, "Microcomputer-based TV-detector for road traffic," Seminar on Micro Electronics for Road and Traffic Management, Tokoyo, Japan, October, 1984.
- [2] P. Anandan, "A computational framework and an algorithm for the measurement of visual motion," International Journal of Computer Vision, vol. 2(3), pp. 283-310, 1988.
- [3] M. Athans, Systems, Networks, and Computation: Multivariable Methods, McGraw-Hill, New York, NY, 1974.
- [4] J. Craig, Introduction to robotics: mechanics and control, Addison-Wesley, Reading, MA, 1985.
- [5] E. Dickmanns, B. Mysliwetz, and T. Christians, "An integrated spatio-temporal approach to automatic visual guidance of autonomous vehicles," IEEE Transactions on Systems, Man, and Cybernetics, vol. 20(6), pp. 1273-1284, November, 1990.
- [6] B. Horn, Robot vision, MIT Press, Cambridge, MA, 1986.
- [7] A. Houghton, G. Hobson, L. Seed, and R. Tozer, "Automatic monitoring of vehicles at road junctions," Traffic Engineering Control, vol. 28(10), pp. 541-453, October, 1987.
- [8] R. Inigo, "Application of machine vision to traffic monitoring and control," IEEE Transactions on Vehicular Technology, vol. 38(3), pp. 112-122, August, 1989.
- [9] B. Kass, A. Witkin, and D. Terzopoulos, "Snakes: Active contour models," International

- Journal of Computer Vision, vol. 1(4), pp. 321-331, 1987.
- [10] N. Kehtarnavaz, N. Griswold, and J. Lee, "Visual control of an autonomous vehicle (BART) — the vehicle-following problem," IEEE Transactions on Vehicular Technology, vol. 40(3), pp. 654-662, August, 1991.
 - [11] M. Kilger, "A shadow handler in a video-based real-time traffic monitoring system," in Proceedings of the IEEE Workshop on Applications of Computer Vision, 1992, pp. 11-18.
 - [12] P. Michalopoulos, "Vehicle detection video through image processing: the autoscope system," IEEE Transactions on Vehicular Technology, vol. 40(1), pp. 21-29, February, 1991.
 - [13] M. Okutomi and T. Kanade, "A locally adaptive window for signal matching," International Journal of Computer Vision, vol. 7(2), pp. 143-162, 1992.
 - [14] N. Papanikolopoulos, P. Khosla, and T. Kanade, "Visual tracking of a moving target by a camera mounted on a robot: a combination of control and vision," IEEE Transactions on Robotics and Automation, vol. 9(1), pp. 14-35, 1993.
 - [15] N. Papanikolopoulos, "Controlled active vision," Ph.D. Thesis, Department of Electrical and Computer Engineering, Carnegie Mellon University, 1992.
 - [16] C. Pellerin, "Machine vision for smart highways," Sensor Review, vol. 12(1), pp. 26-27, 1992.
 - [17] C. Smith, S. Brandt, and N. Papanikolopoulos, "Controlled active exploration of uncalibrated environments," in Proceedings of the IEEE Conference on Computer Vision and Pattern Recognition, 1994, pp. 792-795.
 - [18] M. Takatoo, T. Kitamura, Y. Okuyama, Y. Kobayashi, K. Kikuchi, H. Nakanishi, and T. Shibata, "Traffic flow measuring system using image processing," in Proceedings of SPIE, 1990, pp. 172-180.
 - [19] C. Thorpe, M. Hebert, T. Kanade, and S. Shafer, "Vision and navigation for the Carnegie-Mellon NAVLAB," IEEE Transactions on Pattern Analysis and Machine Intelligence, vol. 10(3), pp. 362-373, 1988.
 - [20] B. Ulmer, "VITA- an autonomous road vehicle (ARV) for collision avoidance in traffic," in Proceedings of the Intelligent Vehicles '92 Symposium, 1992, pp. 36-41.
 - [21] R. Waterfall and K. Dickinson, "Image processing applied to traffic, 2. practical experience," Traffic Engineering and Control, vol. 25(2), pp. 60-67, 1984.
 - [22] T. Zielke, M. Brauckmann, and W. Von Seelen, "CARTRACK: computer vision-based car-following," in Proceedings of the IEEE Workshop on Applications of Computer Vision, 1992, pp. 156-163.



(a)



(b)



(c)



(d)



(e)



(f)

Figure 14: Pedestrian Tracking through Optical Flow



(a)



(b)



(c)



(d)



(e)



(f)

Figure 15: Vehicle Tracking through Optical Flow



(a)



(b)



(c)



(d)



(e)



(f)

Figure 16: Pedestrian Detection through Figure Segments